Time-dependent aspects of electron degradation: Subexcitation electrons in O_2-N_2 mixtures

Mineo Kimura, Ines Krajcar-Bronić,* Thomas H. Teng,† and Mitio Inokuti
Argonne National Laboratory, Argonne, Illinois 60439
(Received 7 February 1992)

The time evolution of subexcitation electron degradation spectra in N_2-O_2 mixtures has been investigated by using the time-dependent Spencer-Fano equation. The calculations were performed for low-energy electrons whose energies fall below 6 eV. The present study showed that strong resonances in vibrational excitation channels in N_2 and O_2 greatly affect the spectrum at early times, and that the stationary spectrum (time $\rightarrow\infty$) is more readily achieved in energy regions with a large stopping power. The evolution of the characteristic features of spectra of pure N_2 and O_2 and their presence to various degrees in mixtures are also discussed.

PACS number(s): 34.80.Gs, 34.50.Bw, 51.10.+y

I. INTRODUCTION

Time-independent aspects of subexcitation electron degradation in pure N_2 and pure O_2 have been studied previously by using the Spencer-Fano (SF) equation [1,2]. The results showed that strong resonance channels have a dominant effect on the degradation process in both gases. Low-lying electronic excitations in O_2 and shape resonance in both N_2 and O_2 are key elements that moderate the electrons' motion. The presence of the Lewis effect—discrete energy losses appearing prominently near the source energy, where collisions are of only a few kinds and become less conspicuous as the number of collisions increases—is also evident in the degradation process.

The present study now extends the previous research to time-dependent aspects of electron degradation in N_2 and O_2 and in O_2-N_2 mixtures [3]. In general, we expect that strong resonance channels will again play an important role in the degradation of electrons, this time also affecting its progress. Their effects can be basically separated into three energy regions. (i) Above 3.5 eV and below the first electronic excitation threshold of N_2 at 6.2 eV, where the electronic excitations of O_2 are dominant and the cross sections of N_2 are small; (ii) between 1.9 and 3.5 eV, where the shape resonance boosts the vibrational excitation cross sections of N_2, while the cross sections of the electronic excitations in O_2 begin to decline; and (iii) below 1.9 eV, where both of the mentioned processes take place only slightly or not at all, and shape resonance occurs for the $(0\rightarrow 1)$ vibrational excitation process in O_2. In some regions, O_2 evidently will contribute more to the degradation process than N_2, and in others the reverse will be true. Competition between all of these processes becomes evident as the concentrations of the gases are varied. Indeed, this study provides many insights into the process of electron degradation and its progress toward a stationary state.

II. THEORY

A full discussion on the SF equation in time-independent and time-dependent cases has been presented previously [4]; therefore, only a brief summary of the theory will be given below.

A. Time-dependent SF equation and its continuous-slowing-down-approximation representation

The time-dependent representation of the SF theory (TDSF) is achieved by introducing the incremental electron degradation spectrum $z(T;t)$. It is defined so that the quantity $z(T;t)dTdt$ represents the increment of path length gained or lost collectively by electrons having energies between T and $T+dT$ during the time interval between t and $t+dt$. Then, if the source spectrum is $u(T;t)$ and the medium consists of a single species at number density n, $z(T;t)$ satisfies the equation

$$\frac{1}{v_T}\frac{\partial z(T;t)}{\partial t}=nK_T z(T;t)+u(T;t)\ . \tag{1}$$

In this equation, v_T is the speed of an electron of kinetic energy T. The symbol K_T represents a linear integral operator that has the dimension of a cross section (cm^2) and represents the net gain and loss of all electrons at energy T and at time t as described previously [4,5].

If we now define the cumulative degradation spectrum $Z(T;t)$ as

$$Z(T;t)=\int_{-\infty}^{t} dt' z(T;t') \tag{2}$$

and similarly define the cumulative source spectrum $U(T;t)$, then $Z(T;t)$ obeys the equation

$$\frac{1}{v_T}\frac{\partial Z(T;t)}{\partial t}=nK_T Z(T;t)+U(T;t)\ , \tag{3}$$

and $Z(T;t)\rightarrow y(T)$ as $t\rightarrow\infty$, where $y(T)$ is the time-independent, or stationary, degradation spectrum.

Equation (3) can be transformed to an integral equation, as was done in Ref. [5]. This conversion is convenient for numerical calculations to obtain stable solution of $Z(T;t)$.

The continuous-slowing-down approximation (CSDA) version of the TDSF [Eq. (3)] can be written as

$$\frac{1}{v_T}\frac{\partial Z(T;t)}{\partial t}=n\frac{\partial}{\partial T}[s(T)Z(T;t)]+U(T;t) \tag{4a}$$

and

$$s(T)=\sum_i E_i\sigma_i(T)\ , \tag{4b}$$

where E_i and $s(T)$ are the mean energy-loss and the stopping cross section. For a monoenergetic, sharply pulsed source, the approximation takes the compact form

$$Z(T_0,T;t)=\frac{\Theta(t-\tau)}{ns(T)}\ , \tag{5}$$

where Θ is a time-dependent, energy-dependent function that is given in detail in Ref. [4]. Θ has the apparent feature that as $t>\tau$, $\Theta(t-\tau)\rightarrow 1$.

The extension to mixtures can be made by defining a cross-section operator for each of the species present. Then, for a binary mixture containing species A and B, which do not interact and have densities n_A and n_B, respectively, $z(T;t)$ satisfies the equation

$$\frac{1}{v_T}\frac{\partial z(T;t)}{\partial t}=n_A K_T^A z(T;t)+n_B K_T^B z(T;t)+u(T;t)\ , \tag{6}$$

where K_T^A is the cross section operator referring to collisions with species A and likewise for K_T^B.

B. Time-dependent yield

When the cumulative degradation spectrum $Z(T;t)$ is known, the cumulative yield $N_i^{(\lambda)}(T_0;t)$ of a process i by the molecules of species λ at time t and initial energy T_0 can be calculated as

$$N_i^{(\lambda)}(T_0;t)=n^{(\lambda)}\int_{T(t)}^{T_0} dT\, Z(T;t)\sigma_i^{(\lambda)}(T)\ , \tag{7}$$

where $\sigma_i^{(\lambda)}(T)$ is the cross section for the process i of the molecular species λ. The integrand of Eq. (7) is termed the cumulative yield spectrum; it provides information about the region of the dominant contribution to the yield. The stationary yield is determined at the limit $t\rightarrow\infty$, or

$$N_i^{(\lambda)}(T_0;t)\xrightarrow[t\rightarrow\infty]{}\bar{N}_i^{(\lambda)}(T_0)\ . \tag{8}$$

III. NUMERICAL PROCEDURES

The cross sections used in the present study were compiled by Itikawa *et al.* [6,7]. They were used in the previous time-independent studies [1–3] of pure N_2 and pure O_2, as well as of mixtures of N_2 and O_2. Figures 1 and 2 display cross sections for N_2 and O_2, respectively. While the cross-section data for N_2 given by Itikawa *et al.* [7] appear to be well established, the cross-section data for O_2 given by Itikawa *et al.* [6] may have to be reconsidered. The O_2 data [6], which are used in the earlier electron degradation studies [1,3] as well as in the present study, are largely based on beam measurements. However, Gousset *et al.* [8] put greater weight on electron-swarm measurements and recommend a considerably different set of cross-section data. Further, Lawton and

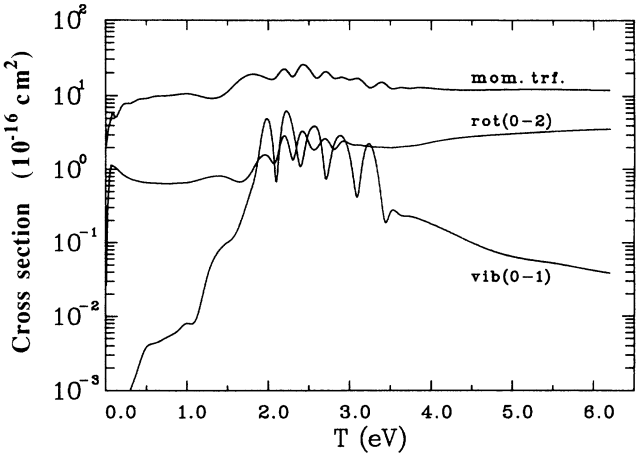

FIG. 1. Cross sections of N_2. mom. trf.: momentum transfer. vib(0−1): (0→1) vibrational excitation. rot(0−2): (0→2) rotational excitation.

Phelps [9] point out that the data of Ref. [6] lead to the energy loss to vibrational excitation being too small to account for electron transport coefficients measured in swarm experiments. To the extent that the O_2 cross-section data are uncertain (as fully discussed in Sec. II B of Ishii, Kimura, and Inokuti [3]), the results of the present work are in part tentative.

Our calculations were carried out for gases maintained at a total pressure of 10 Torr (1.3 kPa) and a temperature of 0 °C. The initial energy of the source electrons was chosen to be 6.0 eV, which is just below the first electronic excitation threshold of N_2. To calculate the cumulative degradation spectrum by solving the TDSF equation we used a time-step size of 0.01 ns and an energy mesh size of 0.01 eV above 1.8 eV and 0.0005 eV below 1.8 eV for all concentrations.

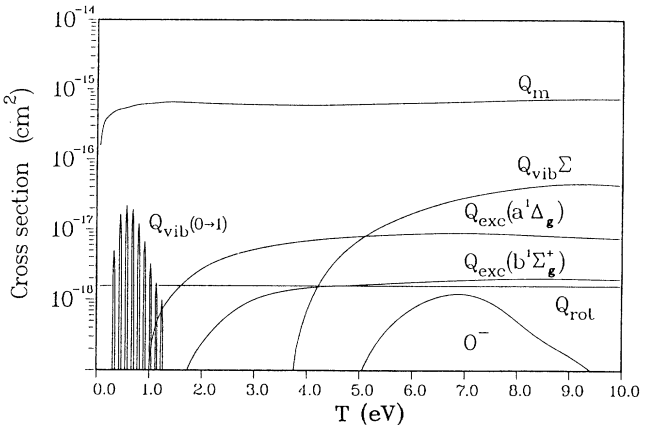

FIG. 2. Cross sections of O_2. Q_m: momentum transfer. $Q_{vib}(0-1)$: (0→1) vibrational excitation. $Q_{vib}\Sigma$: sum of all vibrational excitations. $Q_{exc}(a\,^1\Delta_g)$: $(a\,^1\Delta_g)$ electronic excitation. $Q_{exc}(b\,^1\Sigma_g^+)$: $(b\,^1\Sigma_g^+)$ electronic excitation. Q_{rot}: rotational excitation. O^-: electron attachment. Note that $Q_{vib}\Sigma$ becomes $Q_{vib}(0-1)$ below 1.5 eV.

Stationary spectra can be obtained by solving the time-independent representation of the SF. However, all of the degradation spectra presented here were calculated by using the TDSF method with energy mesh sizes mentioned above. The difference in mesh size above and below 1.8 eV causes different characteristics in the cumulative spectra in the two regions; the lower-energy region is portrayed at an earlier time than its counterpart because a finer mesh size is used there. In spite of this complication, we feel that the use of an especially fine energy mesh size in the lower-energy region is necessary to include the fine resonance structures generated in this region.

IV. RESULTS AND DISCUSSIONS

We will examine the cumulative degradation spectra and the cumulative yield spectra. First, we note the time-dependent and structural features that are present for pure N_2 and pure O_2. Then we treat degradation in mixtures and note the modification of these features as the mixture composition varies.

A. Cumulative degradation spectra for pure N_2 and O_2

Figure 3 shows the cumulative spectra for pure N_2 at various times. At $t=0.2$ ns, the spectrum exhibits regular oscillations and slopes downward as T decreases. The oscillation becomes less evident as time passes; at $t=0.5$ ns it has diminished greatly, and by later times only slight perturbations remain. As expected, the spectrum approaches a stationary state as time passes. The prominent features in the stationary degradation spectrum are (i) small steplike structures between 6 and 3.6 eV and (ii) resonance structures in the region 1.9–3.5 eV. We now examine the physical processes that give rise to these features.

The oscillation that is present in the early degradation spectrum can be attributed to the small number of collisions occurring in the initial stages and the dominance of the vibrational excitation channel. As a result of these two factors, electrons degrade to specific energies upon engaging in vibrational excitations, and prominent peaks appear correspondingly at those energies in the spectrum. The oscillatory structure in the early cumulative spectrum is evenly spaced at intervals of 0.29 eV [that is, the energy loss associated with the $(0\rightarrow 1)$ vibrational excitation process]. The oscillation is a clear demonstration of the Lewis effect during the initial stages of degradation.

The moderation of the oscillation as time passes is caused by an increased number of collisions as the degradation progresses. As more collisions take place, electrons begin to reach a wider range of energies, and weaker channels begin to contribute more significantly to the degradation spectrum. These changes tend to dampen the Lewis effect, and consequently the cumulative spectrum exhibits less of its discrete quality. The Lewis-effect structures were noted in the time-independent study [2] of subexcitation electrons in N_2.

The prominent resonance structures found in the region 1.9–3.5 eV reflect the shape resonance that occurs for all excitation processes in N_2 in this range. Unlike the Lewis-effect oscillations, these structures are not moderated in time, but are a characteristic feature of the N_2 degradation spectrum. For a full discussion of them see Ref. [2]. As we shall see, the shape resonance in this region has a significant effect on the degradation process in the N_2-O_2 mixture.

Figure 4 shows the cumulative spectra for pure O_2. Again, discrete peak structures are evident in the spectrum during the initial stages. At $t=0.2$ ns, large peaks exist at intervals of 0.98 and 1.6 eV, corresponding to excitations to the $a\,^1\Delta_g$ and $b\,^1\Sigma_g^+$ electronic states, respectively. Smaller peaks occur at 0.19-eV intervals because of vibrational excitations, and weaker channels contribute to the jagged appearance of the peaks. Like those of N_2, these features are moderated as the degradation progresses. By $t=10.0$ ns they are barely visible in the degradation spectrum. Indeed, this property is also typical of the cumulative spectra for mixtures, as we will see below.

The dense oscillations superimposed on the regular large oscillations below 1.8 eV arise because the energy

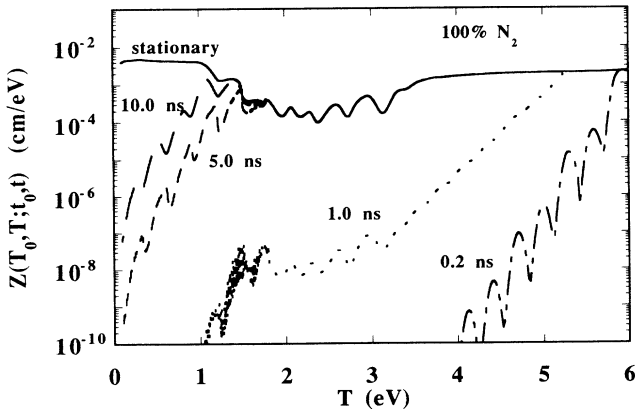

FIG. 3. Cumulative degradation spectra for pure N_2 at various times.

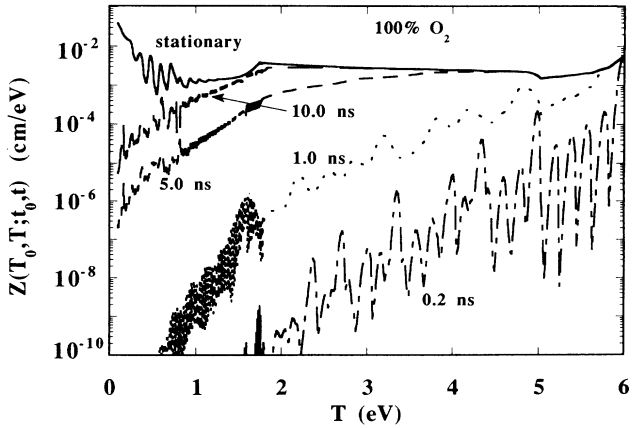

FIG. 4. Cumulative degradation spectra for pure O_2 at various times.

mesh size is smaller in this region. As a result, the spectrum takes into account elastic processes and exhibits closely spaced lines. The spikelike peaks arising from shape resonance in this region are also made conspicuous by the reduced mesh size. They are present from early stages. The resonance structure in the low-energy region is due to the temporary formation of O_2^- [1].

Previous discussions have shown that strong resonance channels have a positive effect on the degradation process. In general, excitation processes involving large energy losses and occurring with high probabilities—and hence contributing to a large stopping power—tend to quicken the rate of degradation. This is clearly seen in Eq. (5), expressed in the inversely proportional relationship between the stopping power and the degradation spectrum in the CSDA. A clear illustration of this reversal in roles can be found by comparing the two pure-case spectra in their initial stages. At $t=0.2$ ns, the cumulative spectrum of N_2 (Fig. 3) is much smaller in magnitude than that of O_2 (Fig. 4), because most of the collisions happening at this time involve electrons with energies up to 4 eV, and the corresponding stopping power of N_2 is weak near the source energy but is increasingly stronger as the energy decreases to 4 eV. Consequently, degradation in N_2 proceeds considerably more slowly than in O_2 at the start, as can be seen in Fig. 5, which represents moderation time as a function of electron energy. However, when electrons degrade to energies in the region 1.9–4.5 eV, where the stopping power of N_2 is about twice as large as that of O_2 and the cross-sectional magnitude of the N_2 $(0\rightarrow 1)$ vibrational excitation is 40 times larger than that of the $a\ ^1\Delta_g$ electronic excitation (the dominant channel in O_2), degradation takes place quickly in N_2 (Fig. 5), and the cumulative spectrum soon reaches equilibrium. In fact, equilibrium is achieved by $t=5.0$ ns for N_2 at energies above 1.8 eV, much earlier than is the case for O_2. In the lower-energy region, however, the cumulative degradation spectrum does not achieve a stationary state so quickly because more collisions are needed for electrons to degrade to those energies, and hence a longer time is needed. This is true for both pure N_2 and pure O_2 and for the mixtures as well.

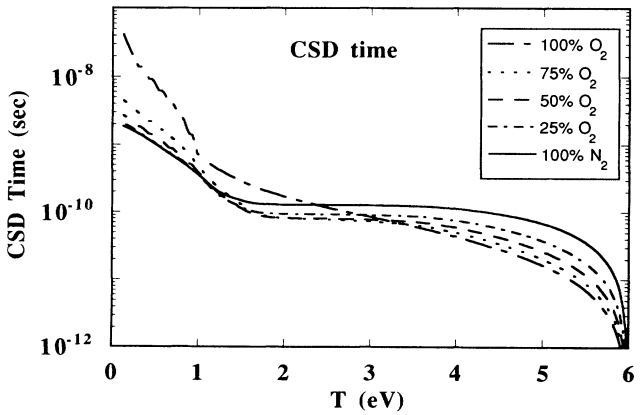

FIG. 5. Moderation time (the CSD time) in pure N_2 and pure O_2 and in mixtures of various compositions as a function of electron energy.

B. Cumulative degradation spectra for N_2-O_2 mixtures

The cumulative degradation spectra for mixtures of various concentrations of N_2 and O_2 are presented in Figs. 6–8 in the order of decreasing O_2 concentration. The general features of the spectra can be understood with the help of previous discussion.

The cumulative degradation spectra for the mixture of 75% O_2 and 25% N_2 are shown in Fig. 6. The spectra still look like that for pure O_2; peaks in the early stage are evident, but they are less distinct because more strong channels are present in the mixture, and the resonance structure is evident in the low-energy region. However, in the middle energy region the sharp resonances in vibrational excitation in N_2 already influence the degradation in this predominantly O_2 mixture. Indeed, the calculation showed that N_2 concentrations as low as 10% still have evident influence in this region, because vibrational excitations in N_2 overwhelmingly dominate any channel in the mixture. In the mixture, the resonance structure of N_2 in the middle energy region is fully conspicuous, although the minima are not as deep as those of the pure N_2 spectrum.

In the 50% O_2+50% N_2 mixture (Fig. 7), and also in the 25% O_2+75% N_2 in Fig. 8, the dense oscillations below 1.8 eV have become much more subdued. This observation is attributed to the sharp drop of the vibrational cross sections of N_2 after electrons pass the resonance region. Hence, the strong vibrational-excitation channels of O_2 have a greater impact on the degradation process. Nevertheless, the overall structure still strongly resembles that for pure N_2.

The degradation spectra for the mixture with 50% O_2 (Fig. 7) and 25% O_2 (Fig. 8) at early times are much more elevated than that for pure N_2 (Fig. 3). This can easily be explained by using the CSDA argument because the presence of O_2 contributes to a large stopping power above the resonance region of N_2. The evolution of the moderation time (the CSD time) [4] as the mixture composition is changed can well be seen from Fig. 5. In the high-energy region, the presence of O_2 in N_2 quickens the degradation process, while in the middle energy region (1.9–3.5 eV) the degradation process is completely defined by the strong nitrogen resonances, even when only small N_2 concentrations are presented in the mixture.

An obvious trend in the spectra is that the resonance structures of N_2 become more prominent as the concentration of N_2 increases, but the sharp resonance peaks of O_2 become less conspicuous. Another progression is that the spectrum reaches equilibrium more quickly as the medium becomes predominantly N_2. Moreover, we may note that the initial Lewis-effect oscillations become increasingly regular. This observation is consistent with our discussions above because fewer energy-loss channels are available to degradation as the O_2 concentration decreases.

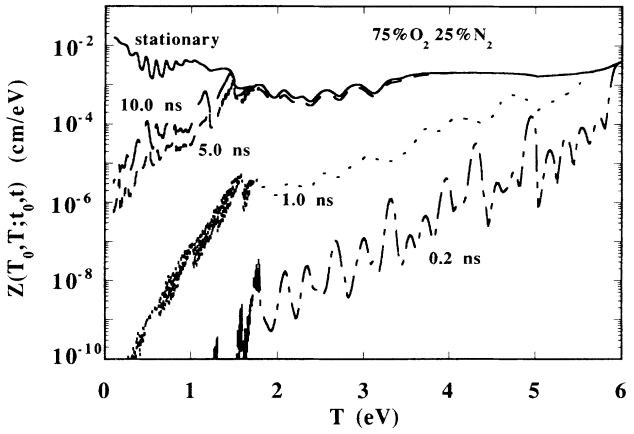

FIG. 6. Cumulative degradation spectra for 75% O_2+25% N_2 at various times.

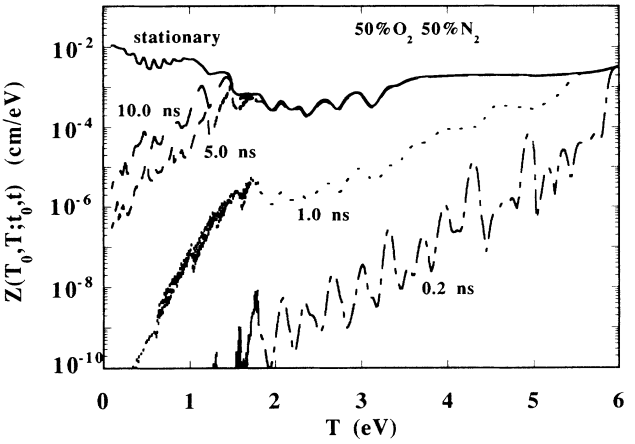

FIG. 7. Cumulative degradation spectra for 50% O_2+50% N_2 at various times.

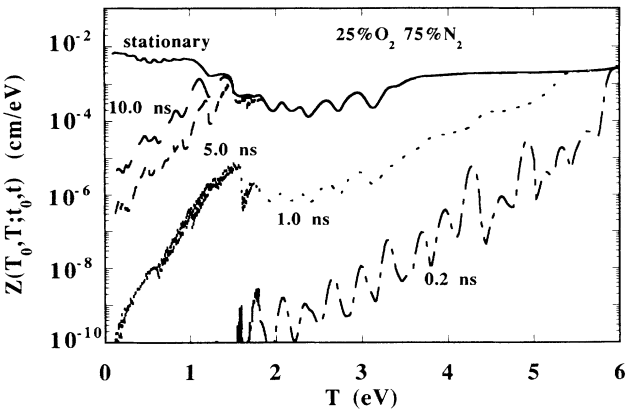

FIG. 8. Cumulative degradation spectra for 25% O_2+75% N_2 at various times.

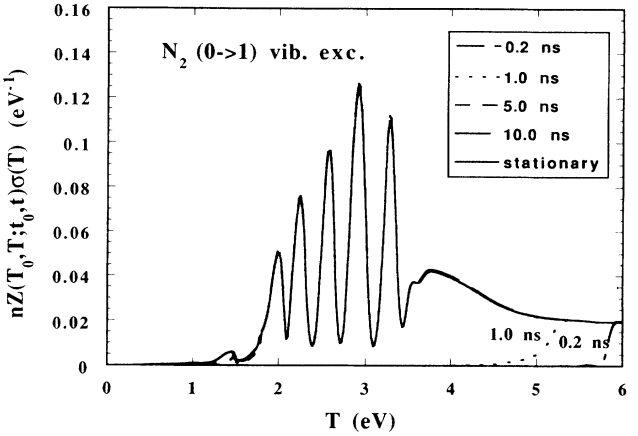

FIG. 9. Cumulative yield spectra for (0→1) vibrational excitation in pure N_2 as a function of time and energy.

C. Cumulative yield spectra

Figure 9 displays the cumulative yield spectra for (0→1) vibrational excitation of N_2. The yield spectra for 5 and 10 ns are nearly identical to that of the stationary state ($t \rightarrow \infty$), except the region below 1.5 eV. As discussed above, the electron reaches the stationary state remarkably quickly. This is a direct consequence of strong

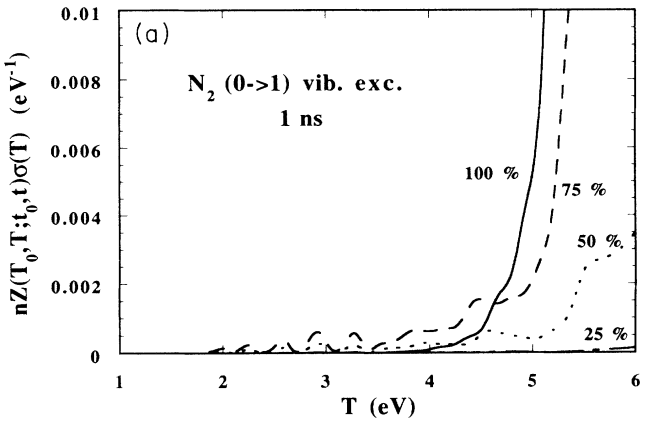

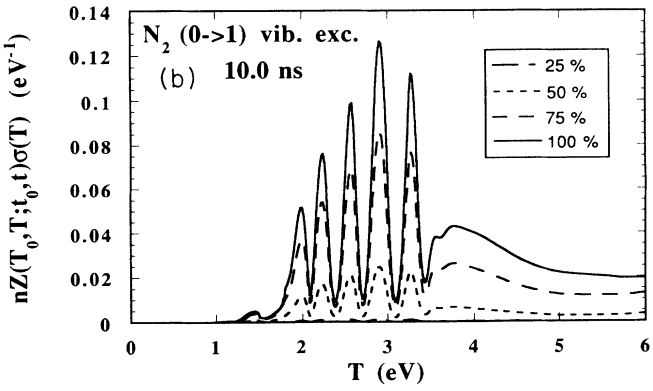

FIG. 10. Cumulative yield spectra for (0→1) vibrational excitation of N_2 in O_2-N_2 mixtures at (a) 1 ns and (b) 10 ns as a function of N_2 concentration.

resonances in the cross sections and hence a large energy-loss process.

The composition dependence of the cumulative yield spectra for (0→1) vibrational excitation is shown in Figs. 10(a) and 10(b) for 1 and 10 ns, respectively. Somewhat surprisingly, the yield spectrum of pure N_2 at 1 ns has smaller values below 4.5 eV than that of 75% N_2 (and the 50% N_2) mixture. This is because the speed of the degradation process in the mixture increases when a small amount of O_2 is introduced, so that the electrons from the high-energy region reach the mid-energy region in a short period of time, causing the reverse of the yield spectrum at early times. However, the area under the curves (corresponding to the yield) appears to be in the normal order (i.e., largest for 100% N_2, second for 75% N_2, and so on).

As was apparent in Fig. 9, 1 ns is quite an early stage of the degradation. When the time reaches 10 ns as in Fig. 10(b), characteristic structures due to the (0→1) vibrational-excitation cross section emerge in the energy region 1.9–3.5 eV, and the order of magnitude of the spectrum is natural relative to the composition.

The cumulative yield spectra for (0→1) vibrational excitation in pure O_2 are displayed in Fig. 11 for various times. Because the degradation process in pure O_2 is slower than that in pure N_2 (as seen in Figs. 4 and 5), even at 10 ns, the yield spectrum has not quite reached the stationary state. This phenomenon is a consequence of weaker energy-loss processes in pure O_2. For clarity, a larger mesh size was used to plot the curves in Fig. 11. Hence, some finer spikelike structures on each larger structure are absent. The cumulative yield spectra as a function of O_2 composition are shown in Figs. 12(a) and 12(b) for 1 and 10 ns, respectively. Below 1.4 eV, the (0→1) vibrational excitation of O_2 is the main contributor to energy loss. Therefore, at any time the order of magnitude of the spectrum is always in the natural order of O_2 composition. At the early time of 1 ns, the spikelike structures in the spectra are obvious. As the time progresses to 10 ns, these structures become large peaks with finer structures on top of each peak. Details of the study of yields for production of each species have been already reported in Ref. [3], and will not be repeated here.

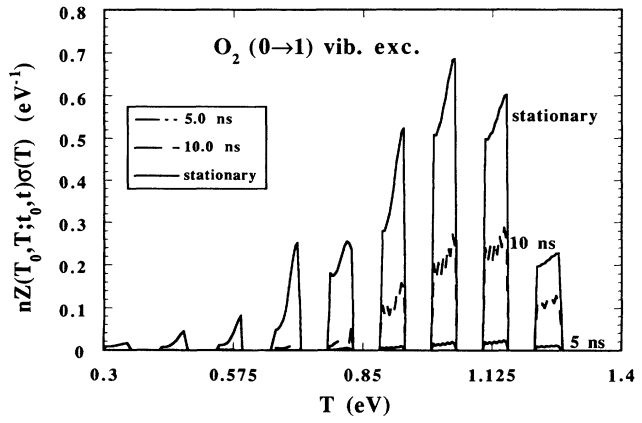

FIG. 11. Cumulative yield spectra for (0→1) vibrational excitation in pure O_2 as a function of time and energy.

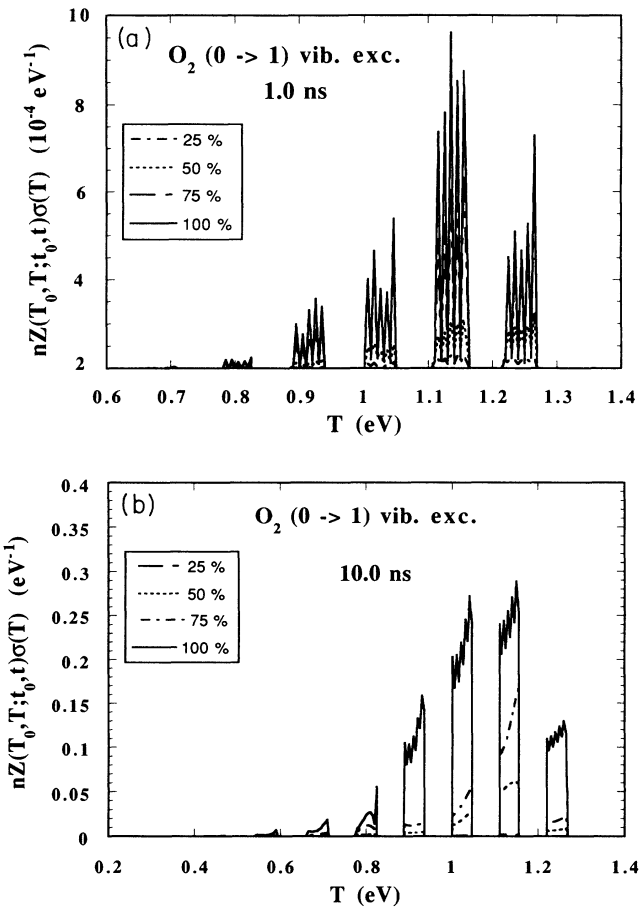

FIG. 12. Cumulative yield spectra for (0→1) vibrational excitation of O_2 in O_2-N_2 mixtures at (a) 1 ns and (b) 10 ns as a function of O_2 concentration.

V. CONCLUSION

We examined the time-dependent aspects of electron degradation in pure N_2 and pure O_2 and in N_2-O_2 mixtures as well. The results showed that degradation proceeds quickly in energy regions where the stopping power is large and less quickly in regions having only weak energy-loss channels. The generation of Lewis-effect structures during the initial stages of degradation is attributed to strong degradation processes, in contrast to the suppressive effect on the spectrum of strong degradation processes in time-independent cases. Strong degradation processes are also attributed to the generation of Lewis-effect structures during the initial stages of degradation, in contrast to the suppressive effect on the spectrum in time-independent cases. Moreover, the progression of prominent structural features, such as resonance oscillations of N_2 in the range 1.9–3.5 eV and sharp reso-

nance peaks of O_2 in the range 0.2–1.3 eV, is also noted in the progression from pure cases to mixtures. We found that the degradation process in mixtures of N_2 and O_2 in the high-energy region and at early times is governed by the O_2, while degradation in the middle energy region is governed by strong resonances in N_2 and degradation in the low-energy region is again governed by O_2.

ACKNOWLEDGMENTS

This work was supported in part by the U.S. Department of Energy, Office of Energy Research, Office of Health and Environmental Research, under Contract No. W-31-109-Eng-38; by Grant No. 1-07-064 from the Ministry of Science and Technology, Republic of Croatia; and by the U.S. National Science Foundation through Research Project No. JF-802/NSF.

*Ruđer Bošković Institute, 41001 Zagreb, Croatia.
†Permanent address: Physics Department, University of California, Berkeley, CA 94720.

[1] M. A. Ishii, M. Kimura, M. Inokuti, and K. Kowari, J. Chem. Phys. **90**, 3081 (1989).
[2] K. Kowari, M. Kimura, and M. Inokuti, J. Chem. Phys. **89**, 7229 (1988).
[3] M. A. Ishii, M. Kimura, and M. Inokuti, Phys. Rev. A **45**, 190 (1992).
[4] M. Inokuti, M. Kimura, and M. A. Dillon, Phys. Rev. A **38**, 1217 (1988).
[5] K. Kowari, M. Inokuti, and M. Kimura, Phys. Rev. A **42**, 795 (1990).
[6] Y. Itikawa, K. Ichimura, K. Onda, K. Sakimoto, K. Takayanagi, Y. Hatano, M. Hayashi, H. Nishimura, and S. Tsurubuchi, J. Phys. Chem. Ref. Data **18**, 23 (1989).
[7] Y. Itikawa, M. Hayashi, A. Ichimura, K. Oda, K. Sakimoto, K. Takayanagi, N. Nakamura, H. Nishimura, and T. Takayanagi, J. Phys. Chem. Ref. Data **15**, 985 (1986).
[8] G. Gousset, C. M. Ferreira, M. Pinheiro, P. A. Sá, M. Touzeau, M. Vialle, and J. Loureiro, J. Phys. D **24**, 290 (1991).
[9] S. A. Lawron and A. V. Phelps, J. Chem. Phys. **69**, 1055 (1978).